Available online at www.sciencedirect.com
ScienceDirect
LWT 41 (2008) 1073–1081
LWT
www.elsevier.com/locate/lwt

Thermal performance of a flat ohmic cell under non-fouling and whey protein fouling conditions

M.A. Ayadi[a,*], T. Benezech[b], F. Chopard[c], M. Berthou[d]

[a]*Unité d'Analyse Alimentaire, Ecole Nationale d'Ingénieurs de Sfax, Route Soukra, BP 3038, Sfax, Tunisia*
[b]*INRA—LGPTA, 369, rue Jules Guesde, 59650 Villeneuve d'Ascq Cedex, France*
[c]*ALFA LAVAL VICARB, rue du Rif Tronchard, 38120 Fontanil Cornillon, France*
[d]*EDF-R&D, Les Renardières, 77818 Moret sur Loing Cedex, France*

Received 15 November 2006; received in revised form 14 June 2007; accepted 21 June 2007

This paper is dedicated to the memory of Dr Jean Claude Leuliet

Abstract

Temperature gradients, between electrode surfaces and bulk, in a continuous flat ohmic cell under whey protein fouling were studied. The temperature profiles in non-fouled cell were studied using two Newtonian fluids (water and an aqueous solution of sucrose at 55 g/100 g) and a pseudoplastic fluid (an aqueous solution of xanthan gum at 0.2 g/100 g). The temperature gradients were studied using two fouling fluids: an aqueous solution of β-lactoglobulin and an aqueous solution of β-lactoglobulin–xanthan gum mixture. Obtained result shows the existence of a temperature difference between electrode surfaces and the bulk when heating non-fouling fluids. The value and the shape of these gradients depend on the Reynolds number and the rheological behavior of the fluid. Under fouling conditions, the temperature gradient obtained at different Reynolds number exhibit a different trend. These differences could be explained by the effect of differential electrical conductivities between the bulk and the deposit, and the balance between heat generation by electrical power dissipation and thermal loss by convection (with the fluid) and conduction (with the electrode surfaces).

Significance for the science community and food industry: Food industry and in particularly the dairy industry, are faced with a severe problem due to equipment fouling during processing. Therefore, the development of alternative technologies for fouling limitation is of scientist and industrial relevance. Ohmic heating is one of these technologies, where the theoretical volume heating aspect should provide a considerable advantage to limit fouling phenomena. The present study evaluates the capability of a rectangular ohmic unit to provide a homogenous heat treatment of complexes dairy fluid (fluid rheology, flow rate and fouling presence).

Keywords: Ohmic heating; Dairy products; Temperature field; Rheology and fouling

1. Introduction

The food industry and in particular the dairy industry, are faced with a severe problem due to equipment fouling during processing. Plate heat exchangers are widely used to achieve pasteurization and sterilization operation. Unfortunately temperature gradient between wall and bulk, due to quite hot wall temperature in conventional heating systems, is known to enhance surface fouling (Belmar-Beiny, Gotham, Paterson, & Fryer, 1993; Lalande, Tissier, & Corrieu, 1985; René, Leuliet, & Lalande, 1991). Such fouling phenomena are one of the biggest constraints with this type of apparatus. The overheating of the deposits formed on the exchange walls may result in the release of undesirable compounds into the product (cooked taste, lactulose, browning, etc.) causing organoleptic alterations. In addition, the development of such deposits may considerably reduce the diameter of the cross-section and create resistance to the heat transfer from the wall to the product, thereby lowering the expected hydraulic and thermal performances of the equipment on the pasteurization or sterilization lines (Changani, Belmar-Beiny, & Fryer, 1997; Delplace & Leuliet, 1995). The complexity of

*Corresponding author. Tel.: +216 21 312 302.
E-mail address: ayadimedali@yahoo.fr (M.A. Ayadi).

0023-6438/$34.00
doi:10.1016/j.lwt.2007.06.022

Nomenclature

Q	dissipated electric power (W)
U	applied voltage (V)
I	electrical current (A)
R	electrical resistance (Ω)
l	thickness (mm)
A	section (mm^2)
Y	cell length (mm)
Z	cell height (mm)
X	cell thickness (mm)
x	x-axis coordinate (mm)
y	y-axis coordinate (mm)
z	z-axis coordinate (mm)
Re	Reynolds number
T	bulk temperature (°C)
$T(y, z)$	bulk temperature in the fourth cell at y, z coordinate (°C)
TC (y, z)	fourth electrode surfaces temperature at y, z coordinate (°C)
ΔT (y, z)	temperature variation between bulk and electrodes surfaces at y, z coordinate (°C)
T^* (y, z)	reduced temperature variation between bulk and electrodes surfaces at y, z coordinate
n	flow behavior index
σ	electrical conductivity (mS/cm)

Subscript

f	fluid
d	deposit
i	inlet
o	outlet
1, 2, 3, 4 and 5	cells number

the fouling reactions, the chemical composition of the products and the parameters involved in the fouling phenomena make modeling and prediction of the phenomena a delicate matter. However, a large number of authors have proposed models to describe milk fouling in tubular and plate heat exchangers. De Jong, Bouman, and Linden (1992) have modeled fouling in the heat treatment of a β-Lg solution. The model was based on the aggregation kinematics of denatured proteins and on wall adsorption reactions. Delplace and Leuliet (1995) have proposed a model for the prediction of the deposit mass in each channel of two Alfa Laval V7 and V13-type plate heat exchangers. The model was founded on a knowledge of the temperature profiles and the degree of β-Lg denaturation. Toyoda and Fryer (1997) have presented a fouling model based on the phenomena of matter transfer between the fluid and the wall. The work was further developed by Georgiadis, Rotstein, and Macchietto (1998), Georgiadis and Macchietto (2000) who added hydrodynamic behavior in the exchanger. Recently, Grijspeerdt, Mortier, De Block, and Renterghem (2004) first formulated and then applied a fouling model to optimize the heat treatment of dairy products using tubular and plate heat exchangers.

Electrical technologies now play a substantial role in this area. Ohmic heating, which appeared at the beginning of the 20th century (Anderson & Finkelsten, 1919), continues to develop both technically and technologically (Amatore, Berthou, & Hébert, 1998; Berthou & Aussudre, 2000; Roberts, Balaban, & Luzuriaga, 1998). The process's strong points (simplicity, reliability, no thermal inertia and volume heating) make it, *a priori*, an effective, durable process to solve or limit fouling problems. Most of the research work done with ohmic technology has focused on tubular devices treating fluids containing particles (Benabderrahmane & Pain, 2000; Eliot-Godéreaux, Zuber, & Goullieux, 2001; Marcotte, 1999; Sastry & Salengke, 1998). A restricted amount of work has been done on the heating of homogeneous fouling fluids (Ayadi, Bouvier, Chopard, Berthou, & Leuliet, 2003; Ayadi, Leuliet, Chopard, Berthou, & Lebouché, 2004a, b).

The objective of this experimental work is therefore to study the evolution of the temperature gradient, between electrode surfaces and bulk, in a flat ohmic cell when heating non-fouling and fouling fluids. The non-fouling study was carried out by heating two Newtonian model fluids and a pseudoplastic one. The fouling study was investigated by heating an aqueous solution of a β-lactoglobulin and an aqueous solution of β-lactoglobulin–xanthan gum mixture.

2. Materials and methods

2.1. Fluids used and their physical properties

Xanthan gum (Degussa E415, Texturant Systems; France), sucrose (Semoule la patissière, France) and whey protein powder (Protarmor 750; Armor protéines; France) were used to formulate fluids tested in this work.

Newtonian fluids were chosen to observe two flow states, i.e. the transition state with a Reynolds number of 1900 (water for a flow rate of 300 l/h) and the laminar state with a Reynolds number of 65 (sucrose solution at 55 g/100 g for a flow rate of 300 l/h).

The pseudoplastic fluid was used in addition to the above Newtonian fluids to determine the temperature profiles in the non-fouled ohmic cell. This fluid was an aqueous solution of xanthan gum at 0.2 g/100 g.

Two fouling model fluids were formulated to study temperature gradient evolution in fouled ohmic cell: (i) an aqueous solution of native whey proteins (1 g/100 g of protein powder) and (ii) an aqueous mixed solution of native whey protein (1 g/100 g) and xanthan gum

(0.2 g/100 g). The choice of these model fluids was based on the fact that the heat denaturation of β-lactoglobulin protein governs milk deposit formation when the temperature exceeds 75 °C (Lalande et al., 1985).

The model fluids were prepared with great care to ensure that their physical properties remained constant for all the tests. To prevent any change to the physical property, model fluids were prepared and stored at 4 °C for 12 h before fouling experiments. Their density, specific heat and thermal conductivity are very close to those of water. The protein–xanthan mixture fluid exhibits shear-thinning behavior characterized by consistency k and flow index n given by

$$n = 0.0023\theta + 0.234, \quad (1)$$

$$k = 6.78\theta^{-0.663}, \quad (2)$$

where θ is the temperature in °C and k is in SI units as dictated by n. These parameters were obtained from regression of data collected over a temperature range of 20–80 °C and shear rates from 0.4 to 700 s^{-1}.

With the temperature range from 10 to 100 °C, the evolution of the electrical conductivity of each fluid was modeled by the following equations.

For the aqueous solution of β-lactoglobulin:

$$\sigma(\theta) = 0.0318\theta + 0.7449. \quad (3)$$

For the aqueous solution of β-lactoglobulin–xanthan mixture:

$$\sigma(\theta) = 0.0363\theta + 0.6762. \quad (4)$$

2.2. Geometry and instrumentation of the ohmic heater

The ohmic heater was made up of an arrangement of five ohmic cells, three of them ensuring heating and the two side cells ensuring electric insulation and the recovery of leakage currents. Each cell can be compared to a rectangular channel ($L = 0.240$ m; $l = 0.75$ m and thickness = 0.015 m), the electrodes constituting side surfaces.

In the case of ohmic heating, the presence of an electrical field makes measurement of the fluid temperature a delicate matter since the sensor may be the seat of electrical energy dissipation by the Joule effect, thereby completely falsifying the measurement results. In addition, the sensor must not disturb the flow since local temperature rise depends on the residence time in the cell and the presence of a recirculation zone or dead zone, even a reduced one, due to the presence of the sensor may lead to erroneous measurements.

Taking into account these constraints, the last heating cell (cell no. 4) of the ohmic module was instrumented with 27 type J iron–constantan thermocouples (diameter 0.001 m). As shown in Fig. 1, 24 thermocouples were implanted on the walls of the cell (12 thermocouples per electrode) so as to obtain a temperature measurement representative of a 15×10^{-4} m^2 surface area.

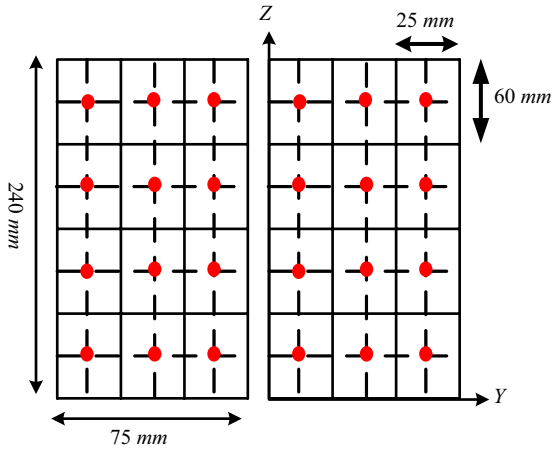

Fig. 1. Thermocouples position on the electrode surfaces of the last heating cell (cell no. 4), ●: thermocouple location.

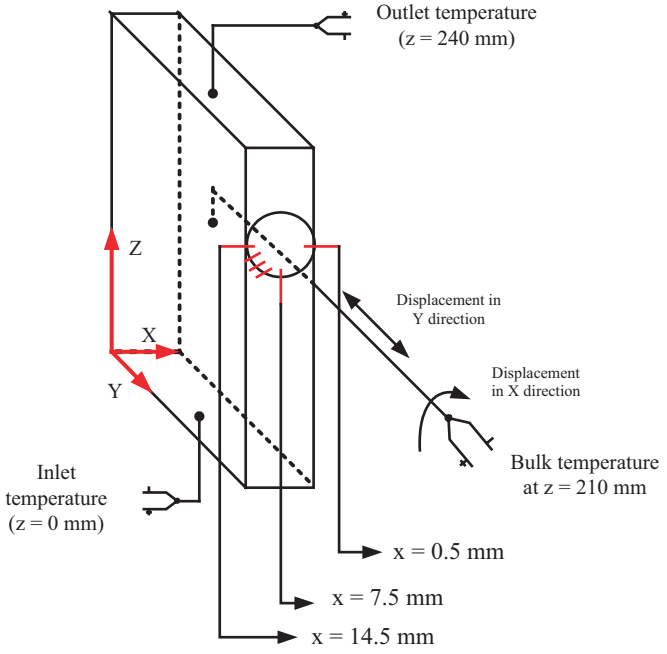

Fig. 2. Bulk temperature measurement in the last heating cell (cell no. 4) of the ohmic module: the system used to insert and move the thermocouple in a measurement section.

The last three thermocouples were coated with a very thin Teflon film (total diameter of thermocouple + sleeve is 0.0012 m) to prevent any Joule effects in them. Two of the three thermocouples were inserted in the inlet and outlet of the cell and the end of the third thermocouple was bent so that the fluid temperature measurement could be taken before the flow was disturbed by the measurement tool. This thermocouple also allows temperature measurements to be taken at any point in the studied section by means of intrusion and movement systems installed at the cell spacer ($Z = 0.21$ m) as shown in Fig. 2. The accuracy of temperature measurements was ±0.2 °C for all the thermocouples.

The reproducibility of the temperature measurement was checked by measuring temperature 3 times in each configuration. The comparisons of these measurements show that the reproducibility does not exceed 5%.

2.3. Fouling trials

The pilot-plant test rig used in the fouling trials is shown in Fig. 3. It consists of three parts: (i) a preheating zone with a plate heat exchanger, (ii) a heating zone with an arrangement of five flat ohmic cells and (iii) a cooling zone with a tubular heat exchanger. In addition, a storage tank ($2\,m^3$), a constant level tank and a volumetric feed pump were necessary to perform the tests. A manual throttling valve at the outlet allowed us to control the backpressure.

The flow rate was measured using an electromagnetic flowmeter (Khrone, type: IFM 10807 K). Temperatures were measured by means of platinum resistance probes (Sensor-Nite, type: Pt 100) placed at the inlet and outlet of each zone. A differential pressure sensor (Schlumberger, type: D) was used to follow the pressure drop increase in ohmic cells. The electric power supply was determined using voltage measurements between the second and third electrodes (Voltmeter 0–250 V, Sineax U504, Chauvin Arnoux) and the intensity of the second phase of the electric transformer (Ammeter 0–200 A, type AC22, Camille Bauer).

All signals were treated (module SCX-1) and collected using a data acquisition card (AT-MOI-16E-10). A software driver (Ni-DAQ) provided the configuration and control of data acquisition system. Data were stored using Labview software systems.

3. Results and discussion

3.1. Temperature profiles in non-fouled ohmic cell

Fig. 4 show the temperature profiles at the ohmic cell outlet ($Z = 210\,mm$) versus cell width ($0 < Y < 75\,mm$) obtained with the three non-fouled fluids at a flow rate of 300 l/h. Fig. 5 shows the temperature profiles at the ohmic cell outlet ($Z = 210\,mm$) versus cell thickness ($0 < X < 12\,mm$) obtained with the three non-fouled fluids at a flow rate of 300 l/h. To be able to compare these results, these temperatures were reduced according to the temperature at the cell's inlet.

These figures indicates that whatever the axis (x or y), whatever the fluid and whatever the flow regime (laminar or turbulent), the fluid near to the wall is always warmer (to varying degrees) than that at the center of the channel.

In the case of water, this temperature gradient did not exceed 2 °C. Consequently, the temperature profile appears flat along the complete measurement section. This result was to be expected, as the flow regime encountered with this fluid is the transitory regime (close to a turbulent regime). This result confirms the results obtained by Muller, Pain, and Villon (1993, 1994) with ohmic heating technology in tubular geometry and those obtained by Ould El Moktar, Peerhossaini, and Bardon (1993) when heating water in a flat ohmic cell.

The sucrose solution is a Newtonian fluid, which is sufficiently viscous to enable the observation of a laminar flow (its viscosity being 15 times that of water). This fluid has the particularity of its viscosity being strongly temperature dependent. This probably implies difficulties

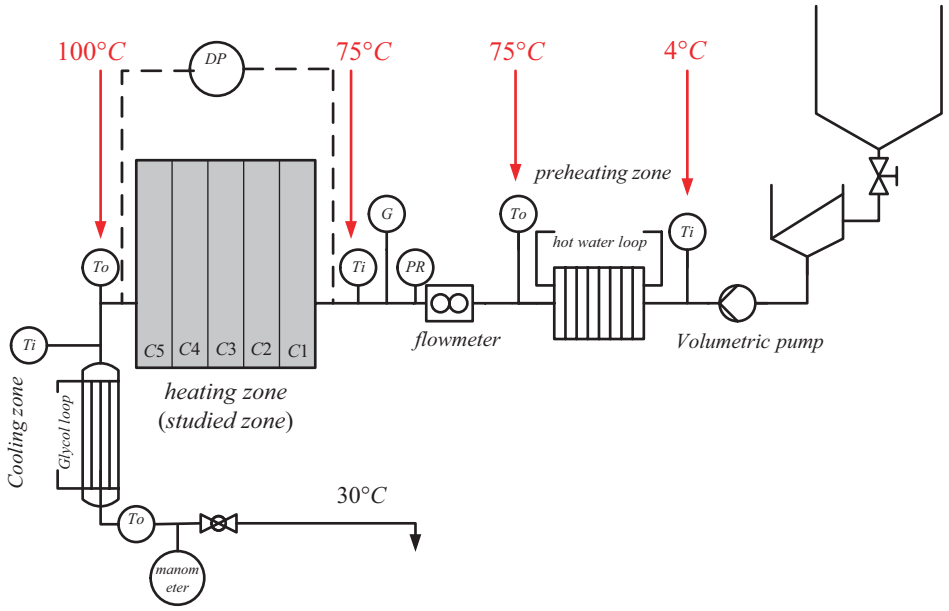

Fig. 3. Pilot-plant test rig, T_i: inlet temperature of each zone, T_o: outlet temperature of each zone, G: electric conductivity, PR: relative pressure and DP: differential pressure.

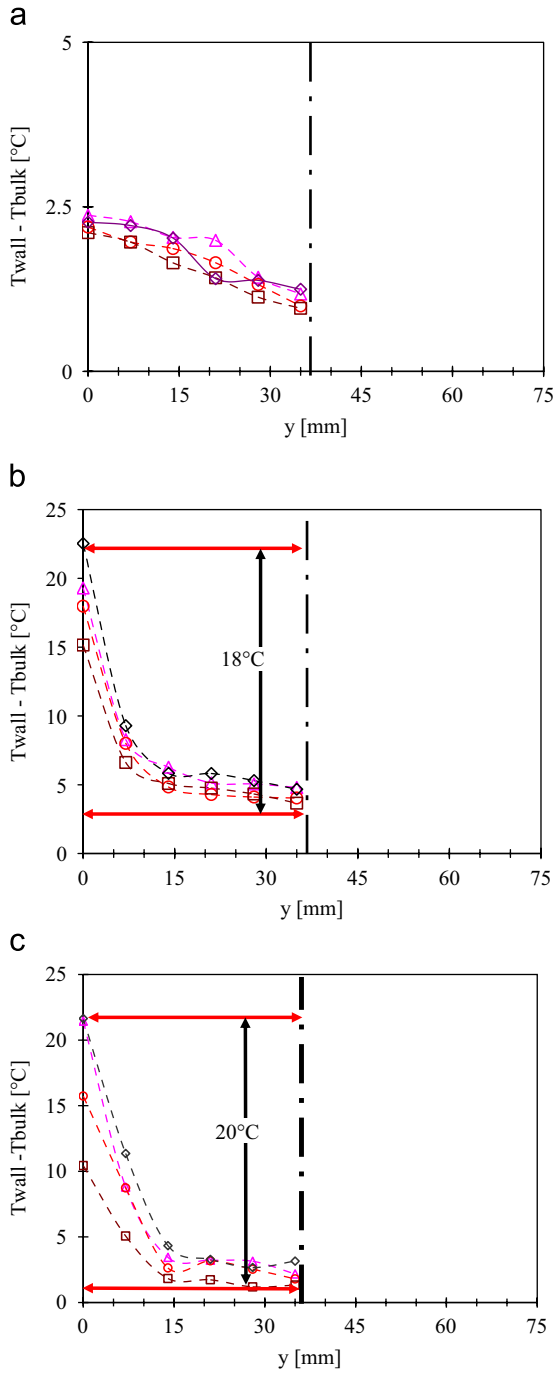

Fig. 4. Temperature profiles at the ohmic cell outlet ($Z = 210$ mm) versus cell width (Y) obtained at a flow rate of 300 l/h: (a) water, (b) aqueous sucrose solution at 55 g/100 g and (c) aqueous xanthan solution at 0.2 g/100 g. (△) $X = 0.5$ mm; (○) $X = 1.5$ mm; (□) $X = 7.5$ mm and (◇) $X = 14.5$ mm.

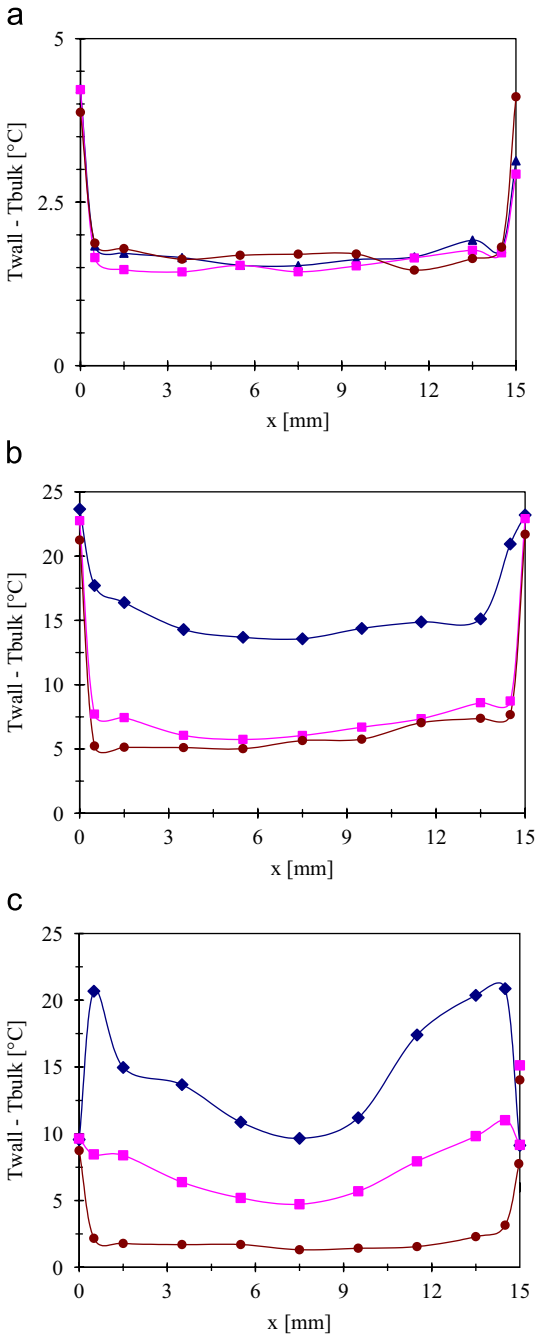

Fig. 5. Temperature profiles at the ohmic cell outlet ($Z = 210$ mm) versus cell thickness (X) obtained at a flow rate of 300 l/h: (a) water, (b) aqueous sucrose solution at 55 g/100 g and (c) aqueous xanthan solution at 0.2 g/100 g. (▲) $Y = 0$ mm; (■) $Y = 7$ mm and (●) $Y = 35$ mm.

in obtaining good homogenization at all temperatures. The temperature gradient between the wall and the center of the channel is almost 9 times that of water. This observation may only be explained by the modification in the general appearance of the velocity profile and consequently in residence time distribution. In effect, the velocity profiles are flattened in the center of the flow, in a turbulent flow regime, (as in the case of water) and forms a parabolic profile in a laminar flow regime (Ayadi et al., 2004b). In the case of the sucrose solution, the velocity is therefore far higher at the center of the channel than at the walls. Fluid particles circulating in the parietal zone are thus submitted to the effects of the electric field for longer periods and are heated to a greater extent than those at the center of the channel. On the other hand, by drawing up temperature profiles along the thickness axis (X) in Figs. 4b and 5b, it was observed that the temperature profile at $y = 0$ mm is significantly different from the others, the fluid was clearly

warmer. These results highlighted the fact that, unlike conditions under turbulent flow regime, in a laminar regime the slowdown in the flow rate in the right angled corners of the rectangular section induced an increase in the fluid temperature, which was significant throughout the entire passage section.

The aqueous xanthan solution presented a pseudoplastic rheological behavior, whose viscosity was close to 15 times that of water for the operating conditions determined for this study (shear rate and temperatures). Figs. 4c and 5c shows that all the y-axis temperature profiles presented a similar appearance to those obtained with the sucrose solution. It should be pointed out, however, that the temperature did not significantly rise from the point where $y = 15$ mm, thereby translating a homogenous temperature throughout the section from 15 to 37 mm. This difference was explained by the lower thermo-dependence of xanthan comparing to that of the sucrose solution. At the wall, the apparent viscosity was lower due to high shear rate conditions. Only 10 °C in the temperature increase was observed compared to 25 °C observed with the sucrose. A deformation in the temperature profiles for $y = 0$ and 7 mm is visible, whatever the thickness. This is translated both by higher temperatures than those recorded for the other planes ($Y = 14$, 21, 28 and 35 mm) and also by a significant heating of the fluid in the vicinity of the walls. The shape of these temperature profiles ($Y = 0$ and 7 mm) could be explained by the buoyancy forces generated by the probable huge differences in the apparent viscosity of this shear-thinning fluid. As for the sucrose solution, we are able to underline the impact of the right angles during the treatment of pseudoplastic fluids by a rectangular ohmic cell.

As fouling phenomena are closely linked to temperature, heterogeneity in the latter may have non-negligible consequences during the treatment of fouling fluids.

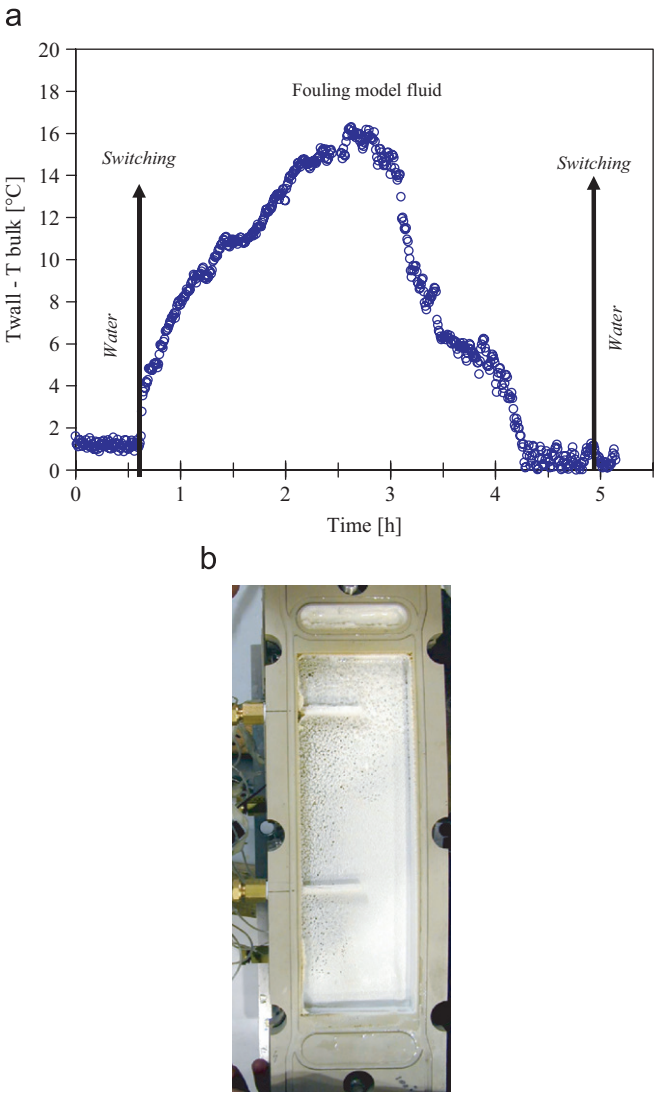

Fig. 6. Measurement of the temperature in the bulk during a 4-h fouling run: (a) evolution of the difference between the wall temperature and the bulk one and (b) photo of the thermocouples in the bulk after the run.

3.2. Temperature profiles in fouled ohmic cell

Fig. 6a shows the evolution of the temperature gradient between the electrode surfaces and the bulk recorded during a 4-h fouling run. It is interesting to note that this figure presents an increase in the parietal temperature during the first 3 h. The latter reaches maximal values and then falls rapidly until it becomes very close to the temperature displayed by the thermocouple in the bulk. This evolution may be explained by the fouling of the thermocouple placed in the bulk. Effectively, it is clear that fouling phenomena are closely linked to flow and to the temperature in the vicinity of the walls. Consequently, at the outset, the electrodes' surfaces become fouled much faster than that of the thermocouple placed in the bulk. The Joule effect of these deposit layers leads to an increase in the temperature of the electrodes. This would, in effect, explain why at the beginning of the run, it was observed a significant difference between the temperatures displayed by the two thermocouples. As the run progressed, the deposit layer which adhered on the thermocouple in the bulk builds up considerably and therefore also become the seat of an electrical energy dissipation due to the Joule effect, inducing an increase in the temperature of the deposit around the thermocouple placed in the bulk. This result thus explained the decrease in the measured temperature gradient so that it practically reached zero (measurement of the Joule effect in both the deposits). In order to illustrate this clearly, Fig. 6b presents the photo of the two thermocouples and the electrode just after a 4 h-fouling run.

Given these results, we can state that it is impossible to observe the evolution in the temperature gradient between the wall and the bulk by measuring the temperature of the fluid with a thermocouple submitted to the effects of an electrical field. This leads us to estimate the temperature in the bulk theoretically, supposing a linear temperature profile between the inlets and outlets of the three heating

cells and the isothermal conditions of the lateral non-heating cells, as reported by Ayadi et al. (2004a).

Taking these hypotheses into account, the temperature gradients between the wall and the bulk in the third heating cell (cell no. 4) are estimated in the following manner. Isothermal hypothesis for the first and the fifth cells:

$$T_i = T_{i1} = T_{o1} = T_{i2} \text{ and } T_o = T_{o5} = T_{i5} = T_{o4}.$$

Linear temperature profile in the ohmic heater:

$$\text{For } z = 0, \quad T_{i4} = T_i + \frac{2}{3}(T_o - T_i). \tag{5}$$

In cell no. 4, for $0 < z < Z$ the local bulk temperature was estimated as follows:

$$T_{z4} = T_i + (T_o - T_i)\frac{z}{Z}. \tag{6}$$

The local temperature variation, between wall and bulk, in cell no. 4, at (y, z) coordinate is

$$\Delta T(y,z) = \mathrm{TC}(y,z) - T_{z4}(y,z). \tag{7}$$

The reduced local temperature variation, between wall and bulk, in cell no. 4, at (y, z) coordinate is

$$T^*(y,z) = \frac{\Delta T(y,z)}{T_o - T_{i4}}. \tag{8}$$

Fig. 7 shows the evolution of the temperature gradient during 4-h fouling experiments. First of all, this figure shows that the gradient between the wall and the bulk does not exceed 2 °C before switching (water), thereby confirming the previously obtained results. Then an instantaneous overheating occurs when heating the fouling fluid formulated with xanthan gum ($Re = 65$). This overheating may be explained by the change in viscosity (change from water to fouling fluid) and consequently the shape of the velocity profile. Hence, it confirmed results obtained during the study of the thermic performances of a non-fouled ohmic cell. In effect, the model fouling fluid was at the same viscosity as the 0.2 g/100 g aqueous xanthan solution previously used. The change-over from water to model fouling fluid caused an increase in the temperature gradient of around 16 °C ($T^* = 2$). After the change-over to model fouling fluid, the local temperature gradient curves present two different evolutions depending on the flow regime.

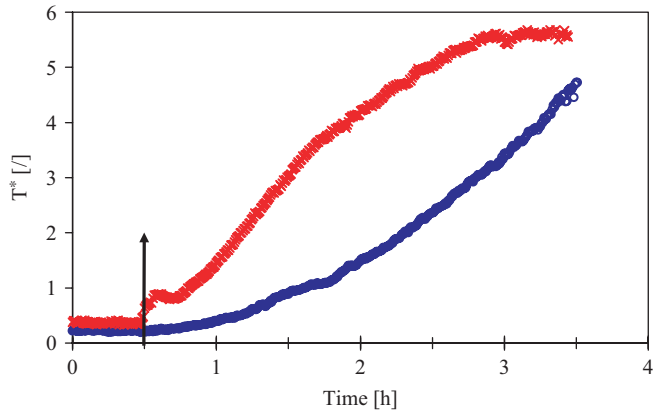

Fig. 7. Reduce local temperature gradient evolution during 4-h fouling runs at $Z = 210$ mm (the temperature in the bulk was estimated, that of the wall was experimentally measured): ($Z = 120$ mm). ×: $Re = 65$; ○: $Re = 1900$.

For the laminar flow, no significant increase in the temperature gradient was visible for a shorter period (the first few minutes of the run). Then a significant increase in the temperature gradient was observed, which reached a high level (7 times the heating value in the cell ≈56 °C). Finally, at the end of the run the curve takes on an asymptotic shape and local temperature gradient disturbances were observed.

As for the laminar flow, in the case of the turbulent flow a very slight increase in the temperature gradient was visible for a shorter period (the first few minutes of the run). Then an exponential evolution was observed.

These curve shapes could be explained as following: during the first few minutes, the deposit was not significant enough to detect a Joule effect in it. So that we do not observe any increase in the temperature gradient. When the deposit became significant it acted as an electrical resistance and the deposit received more and more electrical energy so that its temperature continuously increased. It would be interesting to evaluate the energy dissipation both in the fluid and the deposit. Fig. 8 showed an equivalent electric circuit of a fouled ohmic cell. In the above figure, the resistance of the electrodes is negligible compared to the other components. Then, if a voltage V is applied across the system, we have the following relations.

$$I = \frac{V}{R_d + R_f + R_d} \tag{9}$$

and the voltage drop through the deposit sections is

$$V_d = IR_d = \frac{VR_d}{2R_d + R_f} \tag{10}$$

and the voltage drop through the fluid section is

$$V_f = IR_f = \frac{VR_f}{2R_d + R_f}. \tag{11}$$

Since the current is equal in all cases, the energy generation ($= VI$) within each section (deposit or fluid)

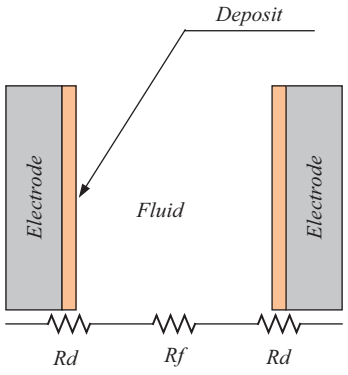

Fig. 8. Equivalent electric circus of fouled flat ohmic cell.

depends only on the applied voltage. Thus:

$$Q_d = V_d I = \frac{V R_d I}{2R_d + R_f} \quad (12)$$

and

$$Q_f = V_f I = \frac{V R_f I}{2R_d + R_f}. \quad (13)$$

Thus:

$$\frac{Q_d}{Q_f} = \frac{R_d}{R_f}. \quad (14)$$

Since

$$R_d = \frac{l_d}{A\sigma_d}$$

and

$$R_f = \frac{l_f}{A\sigma_f}$$

so

$$\frac{Q_d}{Q_f} = \frac{l_d \sigma_f}{l_f \sigma_d}. \quad (15)$$

It is clear that the energy dissipated in both fluid and deposits depend on their relative thickness and electrical conductivities. Ayadi, Leuliet, Chopard, Berthou, and Lebouché (2004c) showed that the electrical conductivity of the deposit is lower than that of the heated fluid and the electric conductivity of the deposit generated by ohmic heating of an aqueous solution of β-lactoglobulin–xanthan mixture is higher than electric conductivity of deposit generated by heating an aqueous solution of β-lactogobulin. Eq. (15), the difference on the deposits electrical conductivities and heat exchange between the deposit and the fluid (convection) and the deposit and the electrode (conduction) could explain the shape of temperature difference observed in Fig. 7. Indeed the deposit generated by heating β-lactoglobulin–xanthan mixture dissipates more electric power than deposit generated by heating β-lactoglobulin solution. Thus, its temperature increases more quickly than the temperature of the β-lactoglobulin deposit. In addition, deposit generated by heating β-lactoglobulin–xanthan mixture exchange less heat by convection than the deposit generated by heating β-lactoglobulin solution (viscosity and properties of each fluid).

4. Conclusions and future work

The study of thermal behavior of a flat ohmic cell when heating fouling and non-fouling fluid, shows that as with conventional heat exchangers, a temperature gradient exists between wall and bulk. In non-fouling conditions, this temperature gradient depends on the flow regime and the fluid rheological behavior. Under fouling condition as soon as deposit phenomenon on the electrode surfaces takes place, it acts as an additional electrical resistance subject to the Joule effect. The dissipation of the electrical energy into the deposit layers causes an increase in its temperatures. It would appear that the evolution in the temperature gradient depends on both the deposit electrical conductivity and the flow regime. Future works will be dedicated to the development of a model for deposit thickness prediction basing on the electrical parameters and the equation developed in this paper.

Acknowledgment

The authors gratefully acknowledge the financial support from Alfa Laval Vicarb and Electricité de France.

References

Amatore, C., Berthou, M., & Hébert, S. (1998). Fundamental principles of electrochemical ohmic heating of solutions. *Ectroanalytical Chemistry*, *457*, 191–203.

Anderson, A. K., & Finkelsten, R. (1919). A study of the electro-pure process of treating milk. *Journal of Dairy Science*, *2*, 374–406.

Ayadi, M. A., Bouvier, L., Chopard, F., Berthou, M., & Leuliet, J. C. (2003). Heat treatment improvement of dairy products via ohmic heating process: Thermal and hydrodynamic effect on fouling. In P. Watkinson, H. Muller-Steinhagen, & M. R. Malayeri (Eds.), *The proceedings of the engineering conference international (ECI): Heat exchanger fouling and cleaning-fundamentals and applications*.

Ayadi, M. A., Leuliet, J.-C., Chopard, F., Berthou, M., & Lebouché, M. (2004a). Ohmic heating unit performance under whey proteins fouling. *Innovative Food Science and Emerging Technologies*, *5*(4), 465–473.

Ayadi, M. A., Leuliet, J.-C., Chopard, F., Berthou, M., & Lebouché, M. (2004b). Experimental study of hydrodynamic behaviour in a ohmic cell: Impact on fouling by whey proteins. *Journal of Food Engineering*, *70*, 489–498.

Ayadi, M. A., Leuliet, J.-C., Chopard, F., Berthou, M., & Lebouché, M. (2004c). Electrical conductivity of whey protein deposit: Xanthan gum effect on temperature dependency. *TransIcheme Part C: Food and Bioproducts Processing*, *82*(4), 320–325.

Belmar-Beiny, M. T., Gotham, S. M., Paterson, W. R., & Fryer, P. J. (1993). The effect of Reynolds number and fluid temperature in whey protein fouling. *Journal of Food Engineering*, *19*, 119–139.

Benabderrahmane, Y., & Pain, J. P. (2000). Thermal behaviour of a solid/liquid mixture in an ohmic heating sterilizer–slip phase model. *Chemical Engineering Science*, *55*, 1371–1384.

Berthou, M., & Aussudre, C. (2000). Panorama sur le Chauffage Ohmique Dans l'Industrie Agro-alimentaire. *Industries Alimentaires and Agricoles*(7/8), 31–38.

Changani, S. D., Belmar-Beiny, M. T., & Fryer, P. J. (1997). Engineering and chemical factors associated with fouling and cleaning in milk processing. *Experimental Thermal and Fluid Science*, *14*, 392–406.

De Jong, P., Bouman, S., & Linden, H. V. D. (1992). Fouling of heat treatment equipment in relation to the denaturation of β-lactoglobulin. *Journal of Dairy Technology Society*, *45*(1), 3–8.

Delplace, F., & Leuliet, J.-C. (1995). Modeling fouling of a plate heat exchanger with different flow arrangements by whey proteins solutions. *Trans Ichem E*, *73*, 112–120.

Eliot-Godéreaux, S., Zuber, F., & Goullieux, A. (2001). Processing and stabilisation of cauliflower by ohmic heating technology. *Innovative Food Science and Emerging Technologies*, *2*, 279–287.

Georgiadis, M. C., & Macchietto, S. (2000). Dynamic modelling and simulation of plate heat exchangers under milk fouling. *Chemical Engineering Science*, *55*, 1605–1619.

Georgiadis, M. C., Rotstein, G. E., & Macchietto, S. (1998). Modelling and simulation of complex plate heat exchanger arrangements under milk fouling. *Computers and Chemical Engineering*, *22*, S331–S338.

Grijspeerdt, K., Mortier, L., De Block, J., & Renterghem, R. V. (2004). Application of modelling to optimise ultra high temperature milk heat exchangers with respect to fouling. *Food Control*, *15*, 117–130.

Lalande, M., Tissier, J. P., & Corrieu, G. (1985). Fouling of heat transfer surfaces related to β-lactoglobulin denaturation during heat processing of milk. *Biotechnology Progress*, *1*, 131–139.

Marcotte, M. (1999). Ohmic heating of viscous liquid food. Ph.D. thesis, Department of Food Science and Agricultural Chemistry, University Mc Gill, Canada.

Muller, F. L., Pain, J. P., & Villon, P. (1993). *Chauffage ohmique des liquides non-Newtoniens* ($6^{ème}$, pp. 229–236), colloque TIFAN, Tome VI.

Muller, F. L., Pain, J. P., & Villon, P. (1994). On the behaviour of non-Newtonian liquids in collinear ohmic heaters. In *Proceedings of the tenth international heat transfer conference* (Vol. 4, pp. 285–290), Brighton, UK.

Ould El Moktar, A., Peerhossaini, H., & Bardon, J. P. (1993). *Effet de la convection naturelle lors du chauffage de fluides complexes par conduction élecrique directe* ($6^{ème}$, pp. 217–228), colloque TIFAN, Tome VI.

René, F., Leuliet, J. C., & Lalande, M. (1991). Heat transfer to Newtonian and non-Newtonian food fluids in plate heat exchangers: Experimental and numerical approaches. *Trans Ichem E*, *69*(Part C), 115–126.

Roberts, J. S., Balaban, M. O., & Luzuriaga, R. Z. D. (1998). Design and testing of a prototype ohmic thawing unit. *Computers and Electronics in Agriculture*, *19*, 211–222.

Sastry, S. K., & Salengke, S. (1998). Ohmic heating of solid–liquid mixtures: A comparison of mathematical models under worst-case heating conditions. *Journal of Food Process Engineering*, *21*, 441–458.

Toyoda, I., & Fryer, P. J. (1997). A computational model for reaction and mass transfer in fouling from whey protein solutions. In *Fouling mitigation of industrial heat exchange equipment*. New York: Begell House.